Journal of Sciences, Islamic Republic of Iran 26(1): 17 - 24 (2015) http://jsciences.ut.ac.ir
University of Tehran, ISSN 1016-1104

The Impact of Cadmium Loading In Fe/Alumina Catalysts and Synthesis Temperature on Carbon Nanotubes Growth by Chemical Vapor Deposition Method

M. Karimi, A. Badiei*, and P. Zarabadi-poor

Department of Chemistry, Faculty of Science, University of Tehran, Tehran, Islamic Republic of Iran

Received: 5 May 2014 / Revised: 27 December 2014 / Accepted: 4 February 2015

Abstract

We evaluated the effect of Fe/Alumina Catalyst contained different Cadmium contents and two synthesis temperatures on producing carbon nanotubes by chemical vapor deposition of methane as a feedstock. X-ray powder diffraction (XRD), N2 adsorption-desorption, scanning electron microscopy (SEM), transmission electron microscopy (TEM), Raman spectroscopy and Thermogravimetry analysis (TGA) were used for characterizing of synthesized catalysts and carbon nanotubes. Raman spectrum confirmed the presence of carbon nanotubes. TGA showed larger deposited carbon nanotubes in certain cadmium contents and higher synthesis temperature of 950 °C. Based on morphological assessment in SEM images, the increase in cadmium content leads to the decrease in diameter of resulted carbon nanotubes

Keywords: Carbon nanotube; CVD; Methane; Cadmium; Fe/Alumina.

Introduction

After the first report of carbon nanotubes (CNTs) discovery by Ijima [1], owing to the unusual structural, electrical, mechanical and thermal properties[2], they become one of the most attractive nanomaterials that fascinated a lot of research groups in the various scientific fields to study their synthesis and potential applications such as catalyst, sensors, nanocomposites, and drug delivery [3-7]. CNTs can be produced with diverse synthesis methods[8], such as arc discharge[9], laser ablation[10] and catalytically chemical vapor deposition (CCVD) [11, 12]. Problems associated with carbon nanotube growth onto large areas and at low temperatures constitute one of the main obstacles for the development of all their potential applications. Chemical vapor deposition is the preferred method with respect to the capability of large scale production, simple and economical procedure, low synthesis temperature requirement and the ability to production different required amounts of CNTs.

CCVD method comprises the growth of carbon nanotubes by decomposition of various hydrocarbons in the presence of metallic catalysts. As a hydrocarbon source, methane, carbon monoxide, acetylene and alcohol are used and Among them, methane is mostly used due to its thermal stability and small self-pyrolysis which causes less formation of amorphous carbon[11]. One of the key parameter to synthesize CNTs by CCVD method is appropriate selection of metals as a catalysts [13]. During catalytic chemical vapor deposition, CNTs grow by the catalytic decomposition of acetylene gas

* Corresponding author: Tel: +982161112614; Fax: +982166405141; Email: abadiei@khayam.ut.ac.ir

over the metal particles. Transition metals have been widely used either in oxide or in metallic forms or as mixtures. Until now, the most investigated catalysts are Fe [14, 15], Ni [16, 17], Co [18, 19]. In addition to using one metal as a catalyst, combination of two different metals have been frequently employed as a catalyst such as Fe/Pt, Fe/Ni, Pd/Cr and etc. The mixture of transition metals was shown to have beneficial effects on the produced CNTs [20-23]. Catalysts are usually supported over solid matrix such as mesoporous silica, alumina and MgO play important rule in growing CNTs. Among those matrix, alumina mainly have been chosen based on high specific surface area, high thermal stability and bonding strongly with catalyst particles, which the last one can hinder metal particle agglomeration [24]. In spite of extensive efforts devoted to obtain carbon nanotubes, optimal conditions of carbon nanotube synthesis have remained under investigation. Moreover, very limited studies have been reported about synthesizing CNTs with metal transition mixture as a catalyst. Therefore, there is still a lot of room to evaluate and insight into of the effects of various combinations of transition metals for producing carbon nanotubes.

Hence, we decided to evaluate the influence of Cadmium loading onto Fe/Alumina catalyst on the growth of CNT in CVD of methane. Fe is well known to be used as a catalyst to synthesis of carbon nanotubes. Here, cadmium in combination with Fe is used to study effects of cadmium in terms of quantity and quality of produced CNTs. We also examined the influence of two synthesis temperatures, i.e. 850 and 950 °C, on the quantity and quality of the obtained CNTs.

Materials and Methods

Materials

The chemicals, including $Fe(NO_3)_3.9H_2O$ (Merck), $Cd(NO_3)_2.4H_2O$ (Merck), Methanol (Merck), Methane (99.99%), and Alumina (Djajarm-Iran, specific surface area : 55 m^2/g) were used as received.

Preparation of the catalysts

Catalysts were prepared according to ref.[15] with some modifications. In all catalysts, the amount of iron salt and alumina were kept constant but the amount of cadmium salt was systemically varied to obtain different Fe-Cd molar ratios. First of all, $Fe(NO_3)_3.9H_2O$ (0.05 M) and a series of $Cd(NO_3)_2.4H_2O$ solutions (0.0125, 0.025, 0.05, 0.1 and 0.2 M) were prepared in methanol. Then, alumina powder (1g) was stirred with 15 ml of $Fe(NO_3)_3.9H_2O$ 0.05M and 15 ml of $Cd(NO_3)_2.4H_2O$ 0.0125M, 0.025M, 0.05M, 0.1M, 0.2M at room temperature followed by evaporating solvent. The resultant solids were dried overnight at 150 °C, grounded into a fine powder. Finally, all catalysts were calcined in air at 500 ºC for 8h. Table 1 provides the list of prepared catalysts along with their corresponding Fe-Cd molar ratios.

Table 1. The list of prepared catalysts and corresponding Fe-Cd molar ratios.

Catalysts	Cd-Fe Molar ratio
$Cd_{0.0125}$Fe/alumina	1:4
$Cd_{0.025}$ Fe/alumina	1:2
$Cd_{0.05}$Fe/alumina	1:1
$Cd_{0.1}$Fe/alumina	2:1
$Cd_{0.2}$Fe/alumina	4:1

Carbon nanotube synthesis

Carbon nanotubes were synthesized according to ref.[15]. Figure 1 shows the schematic representation of the experimental setup. Typically, 0.3 g catalyst powder was placed in a crucible boat within a quartz tube which was located in furnace. Furnace was heated up from room temperature to desired temperature (850 and 950 °C) under argon atmosphere. Once the desired temperature was reached, the flow was switched to the methane for 1h. After that time, furnace was cooled to room temperature under argon atmosphere. Hereafter, we refer to the synthesized CNTs as Cd_xT_y where x represents the Cadmium concentration (in mol/L) and y represents the synthesis temperature.

Characterization methods

N_2 adsorption–desorption isotherms were measured using BELSORP-miniII at liquid nitrogen temperature (-196 °C). All samples were degassed at 300 °C for 3 h under nitrogen gas flow prior to analysis. The specific surface area was calculated using the Brunauer–Emmett–Teller (BET) method. The BJH pore size

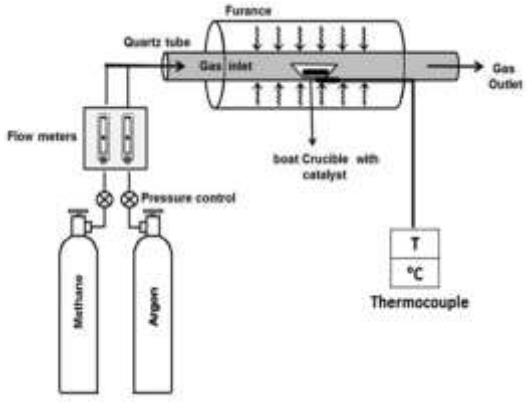

Figure 1. Schematic representation of the experimental setup.

distributions also calculated based on sorption data. X-ray powder diffraction (XRD) patterns were obtained on a Philips X'PERT diffractometer using Cu Kα radiation at 40 kV and 40 mA. Scanning electron microscopy (SEM) was carried out on a LEO 1445V microscope. Transmission electron microscopy (TEM) was performed on a Philips EM208 under an acceleration voltage of 80 kV. Samples were dispersed in ethanol by using an ultrasonic bath, and a droplet of that suspension was placed on a lacey carbon-coated copper grid for analysis. Thermogravimetric analysis (TGA) was carried out in NIETZSCH STA 409 PC/GP instrument from ambient temperature to 1000 °C, using a ramp rate of 10 °C/min. Raman spectra were recorded using a Bruker SENTERRA Raman microscope equipped with a 785 nm laser and CCD detector.

Results and Discussion

Catalyst Characterization

Figure 2 shows the XRD patterns of alumina and catalysts. The patterns of the prepared catalysts are similar to the originial alumina which indicates that the insertion of metal species into the alumina structure unaffect the crystalline structure of alumina in catalysts. Since the intensity of alumina peaks dramatically decreased, we assumeed that the metal particles were substituted in alumina lattice causing the lowering of overall crystallinity of alumina. Furthermore, the most intense peaks attributed to the iron and cadmium oxide are located at $2\theta_{Fe}$ = 33, 34 and 55 and $2\theta_{Cd}$=33, 38 and 55 and these peaks didn't presents in XRD patterns of catalysts because iron and cadmium metals are in small amount in catalysts in comparison with alumina.

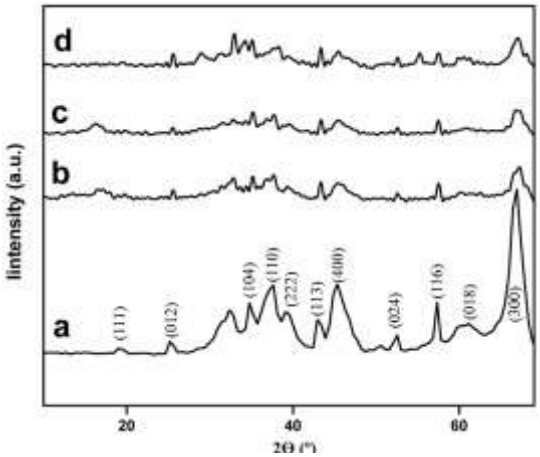

Figure 3. XRD patterns of (a) alumina, (b) $Cd_{0.0125}$Fe/alumina, (c) $Cd_{0.025}$Fe/alumina, (d) $Cd_{0.05}$Fe/alumina.

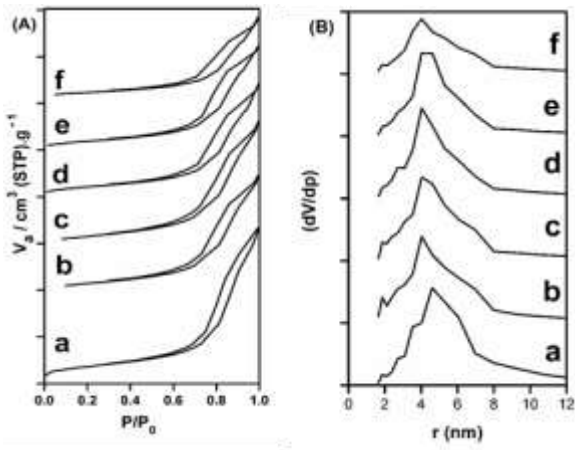

Figure 2. (A) N_2 adsorption-desorption and (B) BJH pore size distributions of (a) alumina, (b) $Cd_{0.0125}$-Fe/alumina, (c) $Cd_{0.025}$-Fe/alumina , (d) $Cd_{0.05}$-Fe/alumina , (e) $Cd_{0.1}$-Fe/alumina, (f) $Cd_{0.2}$-Fe/alumina

Figure 3A shows N_2 adsorption – desorption isotherms of catalysts. As it reported before[15] alumina exhibits a type IV IUPAC standard isotherm implying mesoporosity in alumina. All the catalysts preserved this type of isotherm which confirmed the original structure of alumina in catalysts unchanged during preparation steps. Nevertheless, the increase in cadmium concentrations led to the decrease in the height of the adsorption-desorption isotherms. We explained this observation based on covering of active adsorption sites of alumina by loading metal particles on the surface and into the pores of alumina which resulted in decreasing capability of alumina to uptake the gas.

Table 2 shows the Specific surface area and pore volume of the alumina and catalysts. The insertion of cadmium and iron species into the structure of alumina caused the decrease in the specific surface area and the accessible pore volume of alumina.

Table 2. Structural properties of the catalysts.

Catalysts	SBET (m2/g)	pore volume (cm3/g)	average pore diameter (nm)
$Cd_{0.0125}$-Fe/alumina	45	0.1685	14.923
$Cd_{0.025}$ Fe/alumina	42	0.1580	14.993
$Cd_{0.05}$Fe/alumina	37	0.1503	16.136
$Cd_{0.1}$Fe/alumina	36	0.1404	16.677
$Cd_{0.2}$Fe/alumina	26	0. 1084	16.497
Alumina	52	0.2023	15.477

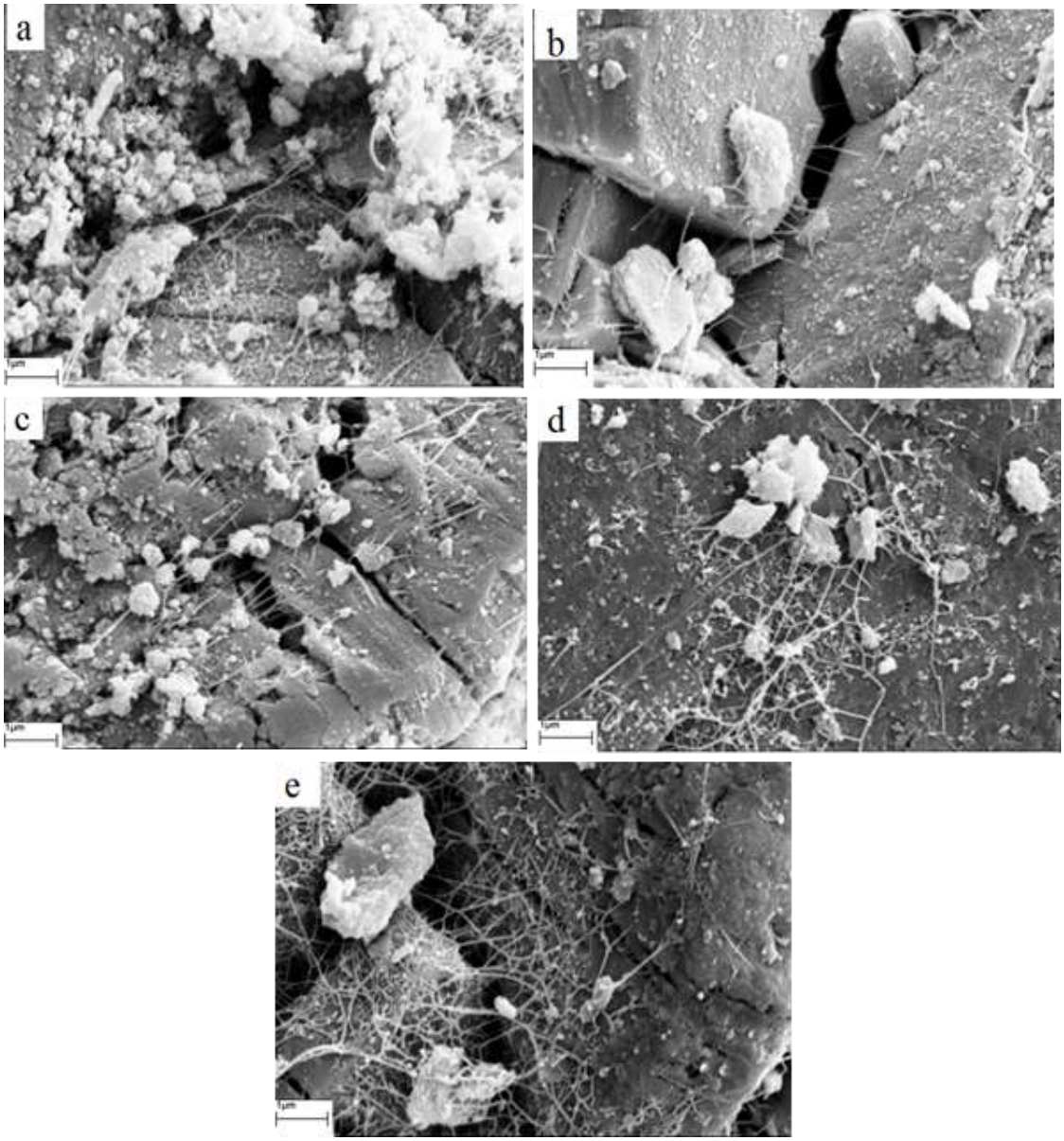

Figure 4. SEM images of (a) $Cd_{0.2}T_{850}$, (b) $Cd_{0.1}T_{850}$, (c) $Cd_{0.05}T_{850}$, (d) $Cd_{0.025}T_{850}$, (e) $Cd_{0.0125}T_{850}$.

Figure 3B presents the BJH pore size distributions of alumina and catalysts. It shows that Increasing in cadmium concentration gradually narrowed and shifted the pore size distributions to the smaller diameters confirming successfully insertion of particles into the pores of alumina in catalysts.

CNT characterizations

We assessed the morphology of produced CNTs by scanning electron microscopy (SEM). Figure 4 and 5 give the SEM images of the prepared CNTs over the catalysts at the synthesis temperatures of 850 and 950 °C for, respectively. As it can be seen, changing both parameters, i.e. synthesis temperature and Cd concentrations, affected the morphology and amount of the deposited CNTs. The higher amount of CNTs was observed at 950 °C. In addition, the complicated morphologies was observed for the synthesized CNTs over catalysts with low Cd contents (Fig5a,b) and the straight CNTs was observed over catalysts with higher content of Cd (Fig5d,e).

Figure 6 provides the corresponding histogram of outer diameter distributions for the samples in Figure 5. The diameter averages of Cd_xT_{950} are 41 nm ($Cd_{0.2}$), 55

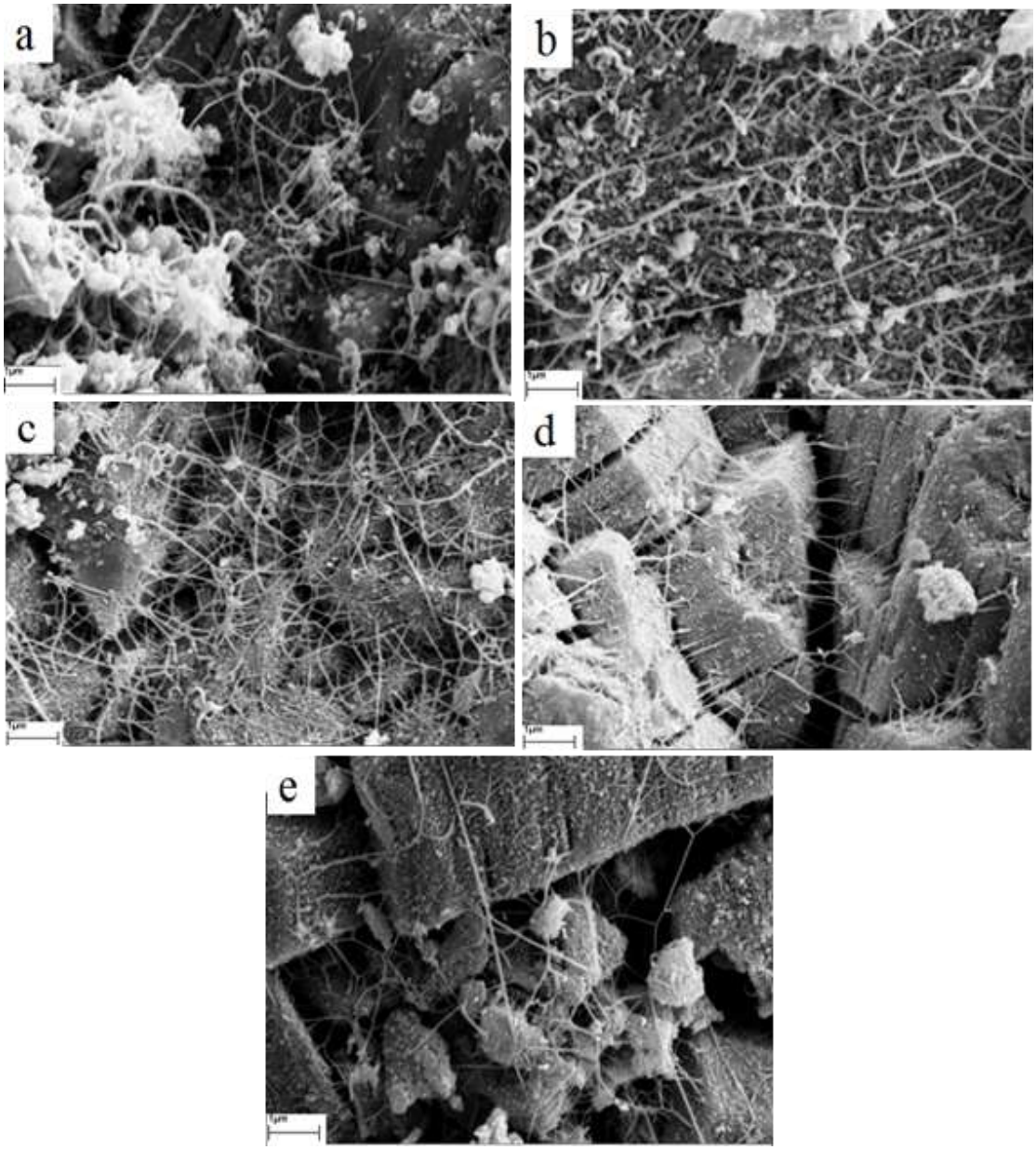

Figure 5. SEM images of (a) $Cd_{0.2}T_{950}$, (b) $Cd_{0.1}T_{950}$, (c) $Cd_{0.05}T_{950}$, (d) $Cd_{0.025}T_{950}$, (e) $Cd_{0.0125}T_{950}$.

nm ($Cd_{0.1}$ and $Cd_{0.05}$), 57 nm ($Cd_{0.025}$) and 62 nm ($Cd_{0.0125}$). As a result, increasing of the cadmium content in catalysts led to the decrease in the average diameter of CNTs. Therefore, we would suggest that cadmium particles could prevent the agglomeration of catalyst particles, because diameter of CNTs is controlled by the size of catalyst particles[25]. The lengths of CNTs in all Cd_xT_{950} were distributed mainly in the range 0.5 – 1 µm. The TEM images of unpurified $Cd_{0.05}T_{950}$ are given in Figure 7. Nanosized particles within nanotubes are seen in this figure that most likely are catalyst particles. Also, the contrast between dark wall and gray inside can prove that synthesized materials are nanotubes and not nanofibers.

Figure 8 shows Raman spectra of the $Cd_{0.1}T_{850}$ and $Cd_{0.1}T_{950}$ samples. The main peak of around 1600 and 1350 cm^{-1} correspond to the G – band (Raman allowed optical mode E_{2g}), an intrinsic feature of carbon nanotubes, and the D – band (originated from disorder in the sp^2-hybridized carbon atoms), attributed to presence defects in the nanotube or the existence of amorphous carbon[26, 27], respectively. The existence of both D and G bonds to gather in Raman spectra confirms that Multi-walled carbon nanotubes were

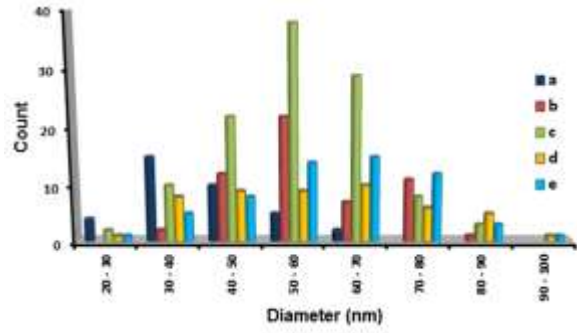

Figure 6. Histograms of outer diameter distributions of (a) $Cd_{0.2}T_{950}$, (b) $Cd_{0.1}T_{950}$, (c) $Cd_{0.05}T_{950}$, (d) $Cd_{0.025}T_{950}$ and (e) $Cd_{0.0125}T_{950}$.

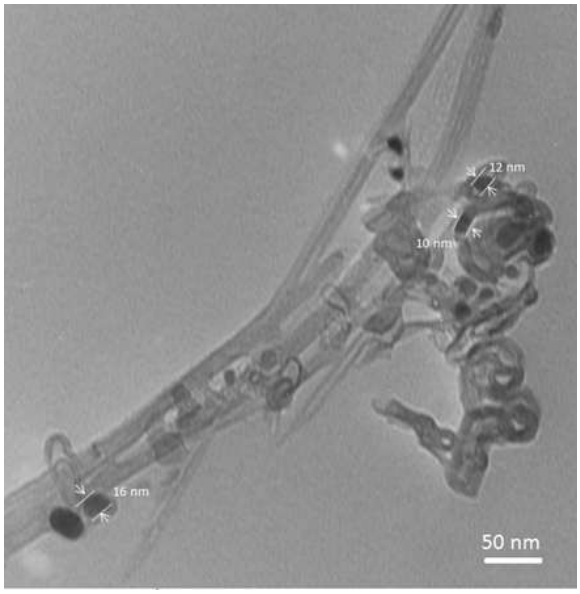

Figure 7. TEM image of $Cd_{0.05}T_{950}$.

produced rather than single-walled carbon nanotubes. It can be due to the size of catalyst particles which they were too large to produce single-walled carbon nanotubes. Furthermore, the intensity of the G-band for synthesized CNT at 950 °C was higher than the one synthesized at 850 °C which indicated the CNT produced at 950 °C might contain more degree of graphitization, i.e. the amount of defects or amorphous carbon in the produced CNTs at 950 °C is smaller than that of produced in 850 °C.

The TGA profiles of the unpurified samples of $Cd_{0.1}T_{850}$ and $Cd_{0.1}T_{950}$ are presented in Figure 9. Typically, the weight losses in the ranges of 300 – 400 °C and T>400 °C are assigned to the elimination of amorphous carbon and to the oxidation of CNTs, respectively. Subtracting of the values of weight loss from T>400 °C to T<700 °C for weight loss percentage on temperature axis of diagrams at were given in Table 3. As it can be seen, the yield of resultant CNTs for Cd_xT_{950} is larger than those of Cd_xT_{850} (Figure 8). It can be proposed that raising reaction temperature to 950 ºC caused in more methane decomposition to the carbon species. Consequently, more carbon species will be available in the vapor phase to diffuse into molten catalyst particles, based on the Vapor-Liquid-Solid

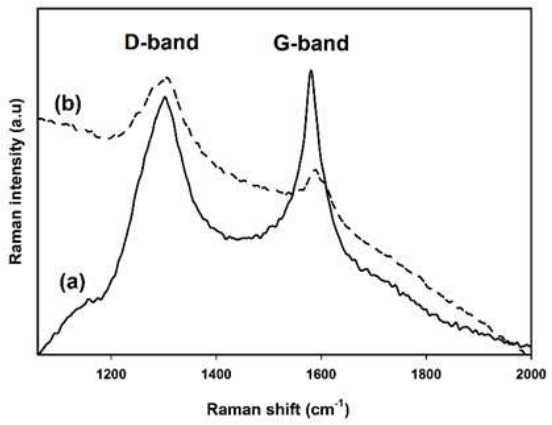

Figure 8. Typical Raman spectrum of (a) $Cd_{0.1}T_{950}$ (solid line) and (b) $Cd_{0.1}T_{850}$ (dash line).

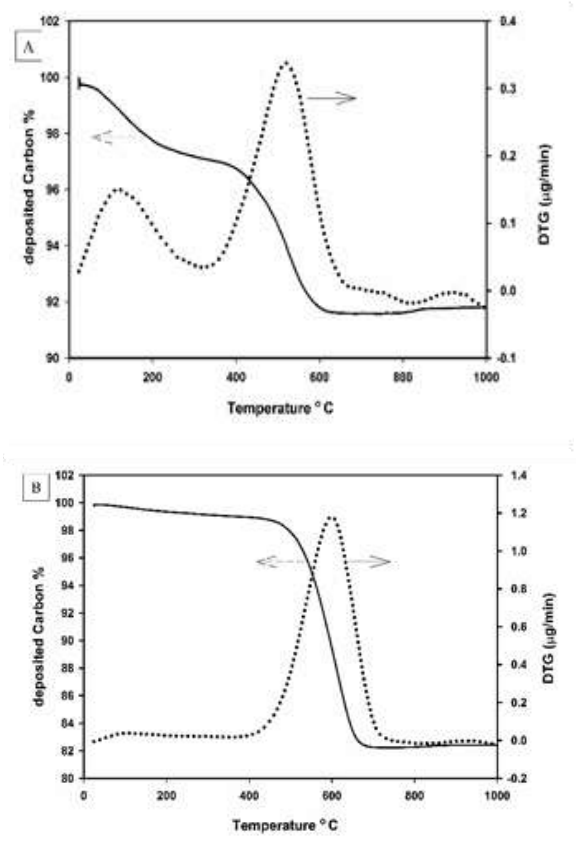

Figure 9. TGA/DTG curves of unpurified samples of (A) $Cd_{0.1}T_{850}$ and (B) $Cd_{0.1}T_{950}$.

Table 6. Percentage of carbon deposition on catalysts.

	Weight loss %	
catalysts	950	850
*Fe/Alumina	16	-
$Cd_{0.2}$Fe/alumina	19	8
$Cd_{0.1}$Fe/alumina	18	7
$Cd_{0.05}$Fe/alumina	17	5
$Cd_{0.025}$ Fe/alumina	12.5	7
$Cd_{0.0125}$Fe/alumina	14.5	4

*based on ref [9] which carried out in our Lab.

(VLS) mechanism[28, 29]. Then, more number of catalyst particles could become activated and get participated in CNTs growth resulting higher amount of CNTs. Furthermore, the yield of resultant CNT was almost increased by increasing Cadmium content of catalysts, so the largest yield of produced CNTs results from $Cd_{0.2}$ with largest cadmium content. It can be supposed that carbon nanotube growth is promoted by cadmium metal. Further, there is not noticeable weight loss in range of 300 – 400° inferred little amorphous carbon produces using methane as carbon feedstock, as it observed in Figure 10.

Conclusion

The use of Fe-Cd/alumina was reported for CNT growth in CVD of methane. The effects of cadmium loading and synthesis temperatures were studied. Cd-Fe/alumina catalysts with different molar ratios of Fe-Cd (4:1, 2:1, 1:1, 1:2 and 1:4) were prepared and characterized by XRD and N_2 adsorption - desorption. Deposited carbon was characterized by SEM and TEM microscopy, Raman spectroscopy and TGA analysis. The SEM images showed that the morphology of as-synthesized CNTs were dependent on the concentration of cadmium metal, e.g. as the concentration of cadmium was increased, the outer diameter of resultant CNTs was moderately decreased. The Raman spectroscopy besides TEM analysis confirmed the successful synthesis of carbon nanotubes. TGA analysis revealed that by increasing cadmium loading (above 1:1 molar ratio), deposited carbon are increased. In respect of largest yield and lowest diameter, $Cd_{0.2}$Fe/alumina catalyst with highest molar ratio of cadmium content was the most active catalyst and the use of $Cd_{0.2}$-Fe/alumina at the synthesis temperature of 950 °C was found to be optimum condition to obtain CNTs. In comparison with reported results of using Fe as a catalyst by Zarabadi-poor and et.al[13], which was done in the same procedures, it does appear that Cadmium make an effective additive, because in the same Fe concentration, the quantity of deposited carbon nanotube over Cd-Fe/Alumina with 0.05 M of Cadmium was increased.

The use other substrate materials such as MCM-41, LUS-1 and SBA-15 which they possess high specific surface area is proposed to study the effect of support structure and pore diameter on the quality and quantity of the synthesized carbon nanotubes in the future works.

Acknowledgement

We would like to thank the University of Tehran research council and Iranian Nanotechnology Initiative for support of this work.

References

1. Iijima S. Helical microtubules of graphitic carbon. *Nature* **354**: 56-58 (1991).
2. Dresselhaus M., Dresselhaus G. and Jorio A. Unusual properties and structure of carbon nanotubes. *Annu. Rev. Mater. Res.* **34**: 247-278 (2004).
3. Schnorr J M. and Swager T M. Emerging Applications of Carbon Nanotubes†. *Chem. Mater.* **23**: 646-657 (2011).
4. Masteri-Farahani M. and Abednatanzi S. New hybrid nanomaterial derived from immobilization of a molybdenum complex on the surface of multi-walled carbon nanotubes. *J. Sci. I. R. Iran* **25**: 27-33 (2014).
5. Gahruei M H. Effective Mechanical Properties of Nanocomposites Reinforced With Carbon Nanotubes Bundle. *Journal of Sciences, Islamic Republic of Iran* **25**: 175-183 (2014).
6. Brahmachari S., Ghosh M., Dutta S. and Das P K. Biotinylated amphiphile-single walled carbon nanotube conjugate for target-specific delivery to cancer cells. *J. Mater. Chem. B.* **2**: 1160-1173 (2014).
7. Noroozifar M., Khorasani-Motlagh M., Hassani Nadiki H., Saeed Hadavi M. and Foroughi M. Modified fluorine-doped tin oxide electrode with inorganic ruthenium red dye-multiwalled carbon nanotubes for simultaneous determination of a dopamine, uric acid, and tryptophan. *SENSOR ACTUAT B-CHEM.* 204: 333-341 (2014).
8. Prasek J., Drbohlavova J., Chomoucka J., Hubalek J, Jasek O., Adam V. and Kizek R. Methods for carbon nanotubes synthesis—review. *J. MATER. CHEM.* **21**: 15872-15884 (2011).
9. Ebbesen T. and Ajayan P. Large-scale synthesis of carbon nanotubes. *nature* **358**: 220-222 (1992).
10. Thess A., Lee R., Nikolaev P., Dai H., Petit P., Robert J., Xu C., Lee Y H., Kim S G., Rinzler A G., Colbert D T, Scuseria G E, Tománek D, Fischer J E. and Smalley R E. Crystalline ropes of metallic carbon nanotubes. *Science* **273**: 483-487 (1996).
11. Kong J., Cassell A M. and Dai H, Chemical vapor deposition of methane for single-walled carbon nanotubes. *Chem. Phys. Lett.* **292**: 567-574 (1998).
12. Li W Z., Xie S S., Qian L X., Chang B H., Zou B S., Zhou W Y., Zhao R A. and Wang G. Large-scale synthesis of aligned carbon nanotubes. *Science*, 1996. **274**(5293): 1701-1703 (1996).

13. Zarabadi-Poor P. and Badiei A. Synthesis of carbon nanotubes using metal -modified nanoporous silicas, in Carbon Nanotubes-Growth and Applications. *M. Naraghi, Editor. InTech: Rijeka* 59-74 (2011).
14. Ermakova M A. Decomposition of methane over iron catalysts at the range of moderate temperatures: the influence of structure of the catalytic systems and the reaction conditions on the yield of carbon and morphology of carbon filaments. *J. Catal.* **201**: 183-197 (2001).
15. Zarabadi-Poor P., Badiei A., Yousefi A., Fahlman B D. and Abbasi A. Catalytic chemical vapour deposition of carbon nanotubes using Fe-doped alumina catalysts. *Catal. Today*. **150**: 100-106 (2010).
16. Ren Z F., Huang Z P., Xu J W., Wang J H., Bush P. and Siegal M P. Synthesis of large arrays of well-aligned carbon nanotubes on glass. *Science* **282**: 1105-1107 (1998).
17. Yudasaka M., Kikuchi R., Matsui T., Ohki Y., Yoshimura S. and Ota E. Specific conditions for Ni catalyzed carbon nanotube growth by chemical vapor deposition. *Appl. Sci. Res.* **67**: 2477-2479 (1995)
18. Hernadi K. Catalytic synthesis of carbon nanotubes using zeolite support. *Zeolites* **17**: 416-423 (1995).
19. Khassin A A,. Yurieva T M. Zaikovskii V I. and Parmon V N. Effect of metallic cobalt particles size on occurrence of CO disproportionation. Role of fluidized metallic cobalt-carbon solution in carbon nanotube formation. *REACT. KINET. CATAL. L.* **64**: 63-71 (1998).
20. Wang X., Yue W., He Mi., Liu M., Zhang J. and Liu Z. Bimetallic catalysts for the efficient growth of SWNTs on surfaces. *CHEM. MATER.* **16**: 799-805 (2004).
21. Ratkovic S., Vujicic D., Kiss E., Boskovic G. and Geszti O. Different degrees of weak metal-support interaction in Fe-(Ni)/Al2O3 catalyst governing activity and selectivity in carbon nanotubes' production using ethylene. *MATER. CHEM. PHYS.* **129**: 398-405 (2001).
22. Ago H., Uehara N., Yoshihara N., Tsuji M., Yumura M., Tomonaga N. and Setoguchi T. Gas analysis of the CVD process for high yield growth of carbon nanotubes over metal-supported catalysts. *Carbon* **44**: 2912-2918 (2006).
23. Atchudan R. and Pandurangan A. The use of bimetallic MCM-41 mesoporous catalysts for the synthesis of MWCNTs by chemical vapor deposition. *J. Mol. Catal. A: Chem.* **355**: 75-48 (2011).
24. Pirard S L., Heyen G. and Pirard J. Quantitative study of catalytic activity and catalytic deactivation of Fe–Co/Al_2O_3 catalysts for multi-walled carbon nanotube synthesis by the CCVD process. *Appl. Catal. A.* **382**: 1-9 (2010).
25. Cheung C L., Kurtz A., Park H. and Lieber C M. Diameter-Controlled Synthesis of Carbon Nanotubes. *J. Phys. Chem. B.* **106**: 2429-2433 (2002).
26. Dresselhaus M S., Dresselhaus G., Jorio A., Souza Filho AG. and Saito R. Raman spectroscopy on isolated single wall carbon nanotubes. *Carbon* **40**: 2043-2061 (2002).
27. Lafi L., Cossement D. and Chahine R. Raman spectroscopy and nitrogen vapour adsorption for the study of structural changes during purification of single-wall carbon nanotubes. *Carbon* **43**: 1347-1357 (2005).
28. Baker R T K., Barber M A., Harris P S., Feates F S. and Waite R J. Nucleation and growth of carbon deposits from the nickel catalyzed decomposition of acetylene. *J. Catal.* **26**: 51-62 (1972).
29. Javey A., Kim H., Brink M., Wang Q., Ural A., Guo J., McIntyre P., McEuen P., Lundstrom M. and Dai H. High-κ dielectrics for advanced carbon-nanotube transistors and logic gates. *Nat Mater.* **1**: 241-246 (2002).